Arrested Swelling of Highly Entangled Polymer Globules

Nam-Kyung Lee,[1,2] Cameron F. Abrams,[3] A. Johner,[1,4] and S. Obukhov[1,4,5]

[1]*Laboratoire Européen Associé ICS(Strasbourg, France)/MPIP(Mainz, Germany)*
[2]*Max-Planck-Institut für Polymerforschung, Ackermannweg 10, 55128 Mainz, Germany*
[3]*Department of Chemical Engineering, Drexel University, Philadelphia, Pennsylvania 19104, USA*
[4]*Institut Charles Sadron, 67083 Strasbourg Cedex, France*
[5]*Department of Physics, University of Florida, Gainesville, Florida 32611, USA*

(Received 27 February 2003; published 6 June 2003)

Upon aging, a collapsed long chain evolves from a crumpled state to a self-entangled globule which can be thought of as a large knot. Swelling of an equilibrium globule in good solvent is a two-step process: (i) fast swelling into an arrested stretched structure with conserved entanglement topology followed by (ii) slow disentanglement. Using computer simulation, we found both mass-mass (m-m) and entanglement-entanglement (e-e) power law correlations inside the swollen globule. The m-m correlations are characterized by a set of two exponents in agreement with a Flory-type argument. The e-e correlations are also characterized by two exponents, both of them larger (by ~ 0.3) than the related m-m exponents. We interpret this difference as evidence of distance-dependent repulsion $E = -0.3\ln(\rho)k_BT$ between entanglements sliding along the polymer chain.

DOI: 10.1103/PhysRevLett.90.225504 PACS numbers: 61.25.Hq, 36.20.Fz, 83.10.Rs

Recently there is an increasing interest in the collapse into and the swelling from a polymer globule [1,2]. These studies are to a large extent inspired by the corresponding challenges of protein folding and denaturation [3]. Although collapse of a homopolymer is now rather well understood [4], the reverse process of swelling of a globule into a polymer coil is much more intricate.

Consider the fully equilibrated (henceforth, "old") globule made of N monomers. The local internal structure of this globule is similar to the structure of a polymer melt with Gaussian correlations ($\langle r_i^2 \rangle \propto i$) for small separations along the backbone. The mean distance between monomers $\langle r_i^2 \rangle$ saturates at the squared globule radius for larger separations. The chain conformation is reflected by the globule boundary, and the chain can be viewed as a sequence of Gaussian strands spanning the globule and comprising $n \propto N^{2/3}$ monomers each [5]. In a large polymer globule, this equilibrium state can be reached only at the expense of many entanglements. These self-entanglements are not compatible with an extended swollen structure and have to be considered as topological constraints to be released upon swelling. This effect is not present in swelling of a freshly collapsed ("fresh") globule [6,7]. The swelling process thus crucially depends on the globule's *age* [8].

In this Letter we examine the structure of an *arrested state*, due to entanglements, which appears in the swelling of an initially equilibrated (old) globule. During swelling, a long chain has to accommodate topological constraints that could freeze the globule in some nearly collapsed state, as originally envisioned by Rabin, Grosberg, and Tanaka [9]. Here, we provide a detailed account of the structure of such a state through a Flory-type argument. To complement our theoretical picture, we present analysis of results of large-scale molecular dynamics (MD) simulation of a swelling globule.

For the simulation, we used a coarse-grained polymer model composed of spherical beads which interact with each other through a truncated and repulsive Lennard-Jones (LJ) potential, and connected to each other along the backbone by harmonic springs. For the simulation presented here, no explicit solvent was considered. Using conventional LJ units of energy ϵ, length σ, and time τ, the Newtonian equations of motion for all particles were explicitly integrated using the velocity-Verlet algorithm [10]. The integration included coupling to a heat bath using a Langevin-type thermostat at $k_BT = 1\epsilon$ with a coupling friction $\Gamma = 0.5\tau^{-1}$ [11]. The potential parameters are chosen such that chain crossings are vanishingly likely, so the self-entangled topology is conserved. The MD simulation began with the growth of a Gaussian random walk of $N = 50\,000$ particles with a step length of 0.97σ, confined within a sphere of radius 22.4σ. The particle excluded volume interactions are then incrementally switched on using a standard warm-up technique [12]. Then, MD integration proceeds with a time step of 0.01τ, and continues until an arbitrary stopping time is reached. The MD time τ is about $1/3$ of the monomer diffusion time $\tau_D = k_BT/D$.

Figure 1 shows the squared radius of gyration R_g^2 for this chain as a function of time. After an initially rapid expansion, the globule size saturates at about $t = 4000\tau$, demonstrating the concept of an "arrested state." Insets in the figure show the radial density profiles at two representative times. As we can see from the snapshot (at $t = 16\,000\tau$) in Fig. 2, the homogeneity perhaps implied by the density profiles is markedly absent. This snapshot, depicting a hemispherical section of the

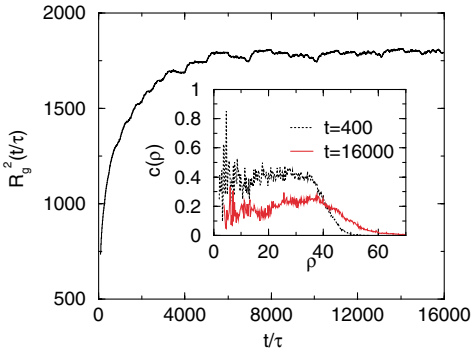

FIG. 1 (color online). Squared radius of gyration during swelling of an equilibrated globule composed of a single chain of length $N = 50\,000$. The inset shows density profiles at two representative times.

arrested globule, shows the highly inhomogeneous nature of the chain conformation.

Our essential point is that the structure of the arrested state is characterized by distinct monomer-monomer correlations and entanglement-entanglement correlations. The initial equilibrium structure can be viewed as an entangled network with one entanglement per every N_e monomers along the chain (in the dense limit). A strand between two entanglements shares space with $\sqrt{N_e}$ similar strands. This defines an "entanglement cell" of initial size $r = \sqrt{N_e}$ (here and below the monomer size is taken as unit length) containing $m = N_e^{3/2}$ monomers and storing an interaction energy $N_e^{3/2}$ (here and below the thermal energy is taken as the energy unit). In the arrested state the globule reaches the optimal swelling compatible with the entanglements. Inside an entanglement cell, the number of monomers m and the number of strands $\sqrt{N_e}$ remains fixed. All strands are forced to stretch alike. The right-hand side drawing of Fig. 2 shows schematically the expanded entanglement cell.

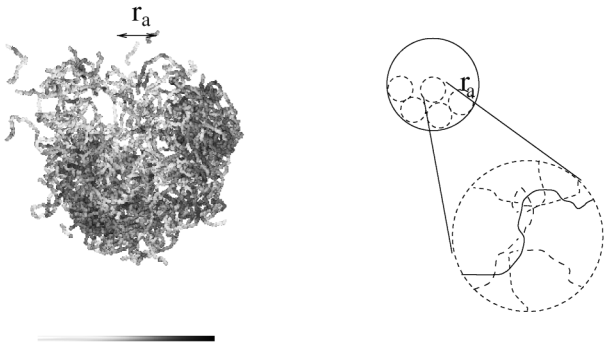

FIG. 2. Snapshot (left) from an MD simulation of a swelling globule ($N = 50\,000$) in the arrested state, showing a hemispherical section of the globule (view from inside out). The entanglement cell size is indicated as r_a. The grey scale depicts the degree of constraint on thermal fluctuations of the monomers (see text). Dark regions indicate the accumulation of entanglements. The accompanying schematic (right) depicts the packing of expanded entanglement cells and their internal structure.

Using a standard Flory argument [13], we can find the equilibrium size and swelling ratio of an entanglement cell. Let r_a be the size of the expanded cell. Balancing the elastic energy of $N_e^{1/2}$ strands per cell, $F_{el} = N_e^{1/2} r_a^2/N_e$, and the excluded volume interaction energy of m monomers per cell, $F_i = N_e^3/r_a^3$, gives the actual cell size in the arrested state as $r_a = N_e^{7/10}$. A similar argument was applied by Pütz *et al.* to describe swelling of cross-linked gels [14], where elasticity is dominated by entanglements but the arrested state is frozen in by the chemical cross-links.

It was noticed in [14] that the scaling dependence $\sqrt{\langle r_i^2 \rangle} = i^{7/10}$ seems to be valid on all scales ($\rho < r_a$). This result is very interesting. Naively one might think that entanglement constraints are important only on the scale of r_a; on smaller scales the strands could, in principle, separate. However, the real-space correlation function $\langle r_{ij}^2 \rangle$ computed from the simulated globule displays a fractal strand structure almost down to the size of an individual monomer, as can be seen in Fig. 3(a). Hence local separation does not occur for strands that cannot cross each other. At each scale r^* of the unexpanded globule the number of different strands is $\propto r^*$ and it remains the same (at least statistically) on the corresponding scale $\rho \propto (r^*)^{7/5}$ in the expanded globule. The previous Flory argument holds at all scales (inside the cell); thus the expansion ratio of scale ρ is $\alpha_\rho = \rho^{2/5}$.

The exponent $\nu_a = 7/10$ describes the internal strand structure via $r_{ij} \sim |i - j|^{\nu_a}$. We observe excellent agreement with $\langle r_{ij}^2 \rangle$ computed from simulation, plotted in Fig. 3(a), which displays a best-fit exponent of 1.44, giving a computed ν_a of 0.72. Note that, in the hypothetical case when local strand separation takes place, one

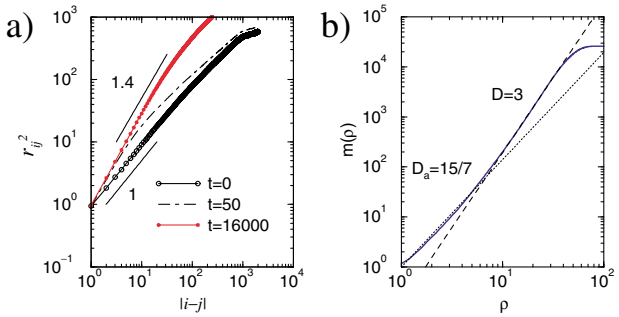

FIG. 3 (color online). Real space correlation functions of a swelling $N = 50\,000$ globule, computed from MD simulations. (a) Single strand correlation functions at $t = 0$, 50, and 16 000 τ (arrested); best-fit value of exponent ν_a from $r_{ij}^2 \sim |i - j|^{2\nu_a}$ is 0.72, and the Flory argument gives $\nu_a = 0.7$ at arrest. (b) Collective Hausdorff dimension of $D_a = 15/7$ and crossover to $D_a = 3$ for the arrested state.

might expect to see two distinct regimes instead: on small scales the swollen chain Flory exponent $\nu = 0.6$, and the exponent 1 characterizing fully stretched strands on a larger scale.

Another quantity which can be directly measured in scattering experiments is the Hausdorff fractal dimension, D_a. It describes the average number of monomers $m(\rho)$ inside the test sphere of radius ρ drawn around a randomly chosen monomer: $m(\rho) \sim \rho^{D_a}$. The contribution from the monomers that belong to the same strand is $\propto \rho^{1/\nu_a} = \rho^{10/7}$. The number of strands scales as $\propto \rho^{5/7}$. The total number of monomers inside of the test sphere is $m(\rho) \sim \rho^{10/7}\rho^{5/7}$. The Hausdorff dimension of the entangled cell should be $D_a = 15/7$ up to scale r_a. At larger scales the globule is a dense packing of cells and the dimension is $d = 3$. The crossover from fractal dimension $D_a = 15/7$ to $d = 3$ is perfectly captured by the simulation results as depicted in Fig. 3(b), where an average is taken over many test spheres and arrested globule configurations.

From the simulation it is possible to gain rough estimates of the cell size m and hence of N_e. We propose $m \approx 160$ and $N_e \approx 30$, which seems not drastically different from typical entanglement lengths in standard melts $N_e^{\mathrm{melt}} \approx 30$–$80$ (N_e and N_e^{melt} are both nonuniversal) [15,16]. The fact that the strands are interpenetrating and strongly correlated inside a cell is nontrivial and sheds new light on the notion of entanglement. An entanglement cannot be thought of either as a strictly local constraint (something like a small ring connecting two strands) nor as a global constraint which reveals itself only on the scale r_a. Our data indicate that the number of strands in any given volume is a statistically conserved quantity under the stretching deformation. It is also clear that the picture incorporated in Flory description is oversimplified: structural disorder seen in Figs. 1 and 2, indicates that some redistribution of entanglements takes place when they slide and aggregate under stress.

In order to visualize the redistribution of entanglements, we calculated for each monomer the average displacement $(\delta\bar{r}_i)^2$ during 100τ. The idea behind this calculation is that, for a strand between two fixed entanglements (or tightened knots), the average square displacement for each monomer is proportional to the distance along the chain to the nearest entanglement (nearest knot). Around the entanglements, the mean square displacements of monomers are small, which allows us to define the effective participation of each monomer in the formation of an entanglement $\beta_i \propto 1/(\delta\bar{r}_i)^2$ (Fig. 2). With this choice of normalization, the sum over entanglement weighted monomers will give the total number of entanglements in the system (with logarithmic accuracy). This number should remain approximately unchanged during redistribution of entanglements. The correlation function of weighted monomer pairs $\Omega(\rho) = \sum_{ij}\langle\beta_i\beta_j\rangle$, where $\rho = |\vec{r}_i - \vec{r}_j|$, shows the fractal structure of entanglements in the arrested state (Fig. 4).

If we count the weighted monomers along a single strand as a function of scale ρ, we obtain the single strand entanglement fractal dimension $1/\nu_a^e = 1.75$. Counting all entanglements inside the sphere of radius ρ gives the multistrand fractal dimension for entanglements $D_a^e = 2.4$. Comparing these exponents with bare monomer-monomer correlation (without weight) exponents $1/\nu_a = 10/7 = 1.43$ and $D_a = 15/7 = 2.14$, we notice the constant difference between these two sets of exponents is about 0.26–0.32. We interpret this difference as a possibility to factor both the single strand and multistrand correlation functions of entanglements as a product of the correlation function of material substrate needed to observe entanglements (monomers) with exponent $10/7$ or $15/7$ and an additional entanglement-entanglement correlation with weight $W(\rho) \sim \rho^{0.3\pm0.04}$. Rewriting this weight in the form $W(\rho) \sim e^{0.3\ln(\rho)}$ we interpret it as pairwise logarithmic repulsive interaction between entanglements: $E = -0.3\ln(\rho)$ (in k_BT units). The logarithmic dependence of the potential is clear from general arguments, as it originates in the entropic nature of the interaction. It is, however, unclear how universal is the prefactor 0.3 and subsequently exponents $1/\nu^e$ and D_a^e; there is an interesting possibility that these exponents are model-dependent. Additional work should be done to resolve this issue.

We point out that no solvent particles were included in the simulations discussed here, which neglects hydrodynamic interactions. Ongoing simulations [8] show that for smaller globules ($N = 512$) with explicit solvent the effect of topology is less dramatic; the swelling is arrested in some stretched intermediate state from which the polymer escapes by a slow, albeit effective, self-disentanglement process. The *transient* regime in the growth of the globule size leading to the arrested state ($t < 4000\tau$ in Fig. 2) depends in general on hydrodynamics, and it is thus not well reflected by the data. In contrast, the arrested state itself, attributed to constraint

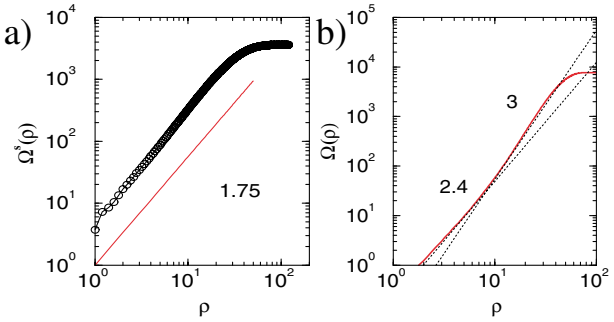

FIG. 4 (color online). Entanglement-entanglement correlation functions, Ω, of the arrested state. (a) Single strand: $1/\nu_a^e = 1.75$; (b) collective Hausdorff dimension of $D_a^e = 2.4$.

equilibrium, is not expected to depend on the details of the solvent-polymer dynamics (e.g., Rouse vs. Zimm).

Below, we demonstrate that the characteristic time in the arrested state τ_d is much larger than the initial expansion time τ_a for long chains. For this purpose it is enough to discuss the chain length dependence. The equilibration of the arrested state is governed by stress diffusion that is characterized by a collective diffusion constant D_c independent of the system size. The time τ_a for the globule swelling to arrest is thus proportional to the squared globule diameter, giving $\tau_a \propto N^{2/3}\tau_D$. To relax out of the arrested state, the globule disentangles with a characteristic time τ_d. The chain ends travel through the entanglements with threading velocity v_d, sliding out of knots, while storing the spared chain length in cells of increasing size. The threading velocity v_d is proportional to the total number of cells $v_d \propto N/\tau_d$. The dissipation rate W_d is dominated by the relative motion of strands inside a cell, $W_d \propto \eta N v_d^2$. On the other hand, the dissipation rate is proportional to total energy dissipated during swelling ($\propto N$) divided by time t_d: $W_d \propto N/\tau_d$. This gives an estimate for the relaxation time $\tau_d \propto N^2\tau_D$. As anticipated, $\tau_d \gg \tau_a$, meaning thermodynamic variables are fast as compared to topological ones. A more detailed analysis restoring powers of N_e [8] does not change this view. Swelling is driven by external forces, which are trying to expand the globule. This explains why the swelling time is shorter than relaxation time of equilibrium globule due to random reptation ($\propto N^3$).

We showed that there is an intermediate arrested state with conserved topology during the swelling of an entangled polymer globule. The arrested state is predicted to have a distinct structure at intermediate scales characterized by a Hausdorff dimension $D_a = 15/7$, which is in perfect agreement with results of direct simulation. This structure hints at some nonlocal effects of entanglements. Nontrivial entanglement-entanglement correlations were found, that can be explained by a (repulsive) logarithmic pair potential between entanglements.

Several light scattering experiments on homopolymer collapse and swelling have been performed by Wu *et al.* [1]. In these studies, the hydrodynamic radius and the radius of gyration are measured during temperature jumps, and their ratio provides an estimate of the globule's compactness. Although these experiments are not time resolved [1], they clear show that large poly(*N*-isopropylacrylamide) globules (10^7 g/mol) are not (completely) arrested and swell back to the coil size. The easiest experimental system to characterize the arrested state may be a weakly cross-linked polymer melt that cannot relax its topology. Furthermore, more recently it has become possible to set up experiments that allow for time resolved synchrotron x-ray diffraction measurements during single molecule collapse, at least for proteins [17]. Stabilizing single synthetic polymers is more challenging. Nevertheless, swelling experiments can be resolved provided single globules are stabilized in the unimer state either thermodynamically (protein-like heteropolymers) or kinetically (charged polymer globules in poor solvent). Although swelling of heteropolymers strongly depends upon the chemical sequence that selects the compact equilibrium state, arrest by topological constraints should be a generic feature.

The authors are grateful for the support from LEA. We thank K. Kremer, M. Rubinstein, and R. Colby for thoughtful discussions.

[1] Chi Wu and Shuiqin Zhou, Phys. Rev. Lett. **77**, 3053 (1996); X. Wang, X. Qiu, and Chi. Wu, Macromolecules **31**, 2972 (1998).
[2] B. Chu and Q. Ying, Macromolecules **29**, 1824 (1996).
[3] O. B. Ptitsyn, Adv. Protein Chem. **47**, 83 (1995), and references therein.
[4] C. F. Abrams, N.-K. Lee, and S. Obukhov, Europhys. Lett. **59**, 391 (2002).
[5] A. Yu. Grosberg and A. R. Khokhlov, *Statistical Physics of Macromolecules* (AIP, New York, 1994).
[6] In the fresh made globule, the average squared geometrical distance between two monomers a distance i apart along the chemical sequence is $\langle r_i^2 \rangle \propto i^{2/3}$. It can also be seen from molecular dynamics (MD) simulation results.
[7] Molten ring polymers adopt crumpled structures in equilibrated simulations, J. P. Wittmer (private communication)
[8] N.-K. Lee, C. F. Abrams, S. P. Obukhov, and A. Johner (to be published).
[9] Y. Rabin, A.-Y. Grosberg, and T. Tanaka, Europhys. Lett. **32**, 505 (1995).
[10] W. C. Swope, H. C. Andersen, P. H. Berens, and K. R. Wilson, J. Chem. Phys. **76**, 637 (1982).
[11] K. Kremer and G. S. Grest, J. Chem. Phys. **92**, 5057 (1990).
[12] C. F. Abrams and K. Kremer, J. Chem. Phys. **115**, 2776 (2001).
[13] P. J. Flory, *Principles of Polymer Chemistry* (Cornell University, Ithaca, NY, 1979).
[14] M. Pütz, K. Kremer, and R. Everaers, Phys. Rev. Lett. **84**, 298 (2000).
[15] M. Doi and S. F. Edwards, *The Theory of Polymer Dynamics* (Oxford Scientific Publications, Oxford, 1986).
[16] M. Pütz, K. Kremer, and G. S. Grest, Europhys. Lett. **49**, 735 (2000).
[17] S. Hagen, J. Hofrichter, A. Szabo, and W. A. Eaton, Proc. Natl. Acad. Sci. U.S.A. **93**, 11615 (1996).